KFUPM
Journal of Undergraduate Research International

Diamond Open Access 164

Article Petroleum Engineering

Impact of Cation Dissolution on Kinetics of CO_2 Mineralization in Carbonate Rocks

Turki Aljuaid and Dhafer Al Shehri*

Cite https://doi.org/10.64589/juri/221334

Submitted: March 02, 2026 **Revised:** March 31, 2026 **Accepted:** April 04, 2026

ABSTRACT

There is a growing need for technologies that mitigate emissions associated with the continued use of fossil fuels. Carbon capture and storage is a promising large-scale CO_2 mitigation approach. However, the kinetics of mineral dissolution and its impact on solution chemistry and subsequent mineralization potential during early reaction stages remain poorly constrained. This study examines the dissolution kinetics of carbonate rocks under high-pressure brine and brine–CO_2 conditions in the context of geological carbon dioxide (CO_2) storage and mineralization. The primary aim of the study is to quantify the lithology-dependent chemical responses and early-time dissolution behavior under controlled subsurface-like conditions. Experiments were conducted using limestone and dolomite core plugs placed in sealed reaction cells at 2000 psi and 75 °C, with time-resolved measurements of pH and dissolved cation concentrations. Early-time calcium release rates were quantified using concentration–time slopes and were normalized by the geometric surface area to enable direct kinetic comparisons across systems. The results showed systematic differences between lithologies and fluid conditions. Dolomite systems exhibit stronger buffering capacity and higher effective dissolution rates than limestone under brine-only conditions, whereas the presence of CO_2 lowers the initial pH and alters early-time calcium mobilization in a lithology-dependent manner. These trends suggest that the early reaction stages are governed by the kinetics before the onset of progressive pH buffering. Overall, the findings provide quantitative insights into the carbonate dissolution behavior under CO_2-rich conditions and support an improved understanding of mineral–fluid interactions relevant to subsurface CO_2 storage and mineralization strategies.

Keywords: carbonate dissolution, CO_2–brine systems, dissolution kinetics, fluid–rock interactions, geological CO_2 storage

1. INTRODUCTION

There is an increased global interesting reducing carbon emissions owing to the increasing impact of greenhouse gas emissions and projections of worsening climate effects without effective mitigation strategies [1,2]. Although international efforts have increasingly emphasized emission reduction and carbon removal strategies, fossil fuels are expected to remain a major component of the global energy mix for decades [3,4]. This highlights the need for technologies that mitigate emissions associated with the continued use of fossil fuels.

Carbon capture and storage (CCS) in deep geological formations is widely recognized as a promising large-scale CO_2 mitigation approach owing to their substantial storage capacity [5]. Several trapping mechanisms contribute to long-term CO_2 retention in subsurface environments, among which solubility trapping and mineralization are considered the most significant [6]. Mineralization is often regarded as the most secure mechanism because it permanently converts CO_2 into stable carbonate minerals [7,8]. Solubility trapping involves the dissolution of injected CO_2 into the formation brines, a process that is strongly influenced by pressure, temperature, salinity, and brine pH [9]. Dissolved CO_2 lowers the brine pH, generating mildly acidic conditions that can promote mineral dissolution, particularly in carbonate reservoirs [10]. This dissolution is an important precursor to mineralization because it releases dissolved divalent cations such as Ca^{2+} and Mg^{2+} into the solution. These cations may contribute to carbonate precipitation and mineral trapping as the system evolves. Moreover, mineral trapping depends on the availability of divalent cations such as Ca^{2+} and Mg^{2+}, supplied either by the brine or released from the reservoir rocks through dissolution [8]. Therefore, in practice, solubility trapping, carbonate dissolution, and mineralization are dynamically coupled processes governed by mineralogy, fluid composition, and reaction kinetics [6,8].

Previous studies have reviewed the trapping mechanisms and mineralization pathways in geological CO_2 storage systems [5–8], investigated pore-scale evolution and geochemical alterations in carbonate reservoirs during CO_2–brine interaction [10–12], and quantified the dissolution kinetics of carbonate minerals under different CO_2 conditions [13–15]. These studies have shown that the carbonate dissolution behavior is strongly influenced by mineralogy, fluid composition, saturation state, and reaction conditions, and that dissolved cation release plays an important role in controlling fluid chemistry and the subsequent mineralization

Table 1. *Summary of related studies and gaps addressed in this work*

Reference	System / Scale	Main focus	Key relevance	Remaining gap
5–8	Reviews / geological CO_2 storage systems	Trapping mechanisms, mineralization pathways, and CO_2 storage processes	Establishes the importance of solubility trapping and mineralization	Broad reviews; no direct early-time limestone–dolomite comparison
10	Carbonate and sandstone reservoirs / pore scale	CO_2–brine interaction and pore-scale evolution	Shows geochemical alteration during CO_2–brine–rock interaction	Pore-scale focus rather than controlled core-scale comparison
11	Carbonate rocks / experimental system	Rock response to CO_2-related interaction	Supports experimental study of carbonate response to CO_2	Focuses on rock-property response rather than kinetic lithology comparison
12	Carbonates / pore scale or fundamental properties	Carbonate behavior under reactive conditions	Provides background on carbonate behavior in reactive systems	Foundational background, not a direct comparative reactive study
13,14	Carbonate minerals and carbonate rocks / kinetic and experimental studies	Dissolution kinetics and CO_2-related carbonate reactivity	Provides kinetic background for carbonate dissolution under CO_2 conditions	Focus on mineral-scale or process-specific behavior
15	Carbonate rocks / microstructure	Localized versus distributed dissolution and role of microstructure	Highlights the role of rock structure in dissolution behavior	Emphasizes microstructure rather than bulk lithology response
This study	Limestone and dolomite core plugs / core scale	Early-time dissolution kinetics under brine-only and brine–CO_2 conditions	Direct comparison of pH evolution, cation release, and early-time Ca dissolution	Addresses the lack of direct core-scale limestone–dolomite comparison

behavior[10,12,13,15]. Collectively, these studies provide important insights into carbonate dissolution, CO_2–brine interactions, and mineral–fluid behavior relevant to geological CO_2 storage.

However, the available literature mostly focuses on general trapping mechanisms, equilibrium behavior, long-term geochemical evolution, and mineral- and pore-scale processes[5,6,8,10,12]. Quantitative experimental data on early-time cation dissolution kinetics remain limited, particularly at the core scale and for direct comparisons between limestone and dolomite under the same controlled brine-only and brine–CO_2 conditions. In particular, variations in previous studies in terms of scale, lithology, and experimental focus have obscured the specific research gap . Although the thermodynamic behavior of CO_2–brine systems is relatively well established, the kinetics of mineral dissolution and its impact on solution chemistry and subsequent mineralization potential during early reaction stages remain poorly understood. This is important because early-stage kinetics determine how rapidly the brine approaches saturation and the consequent initiation of mineralization processes, which may also affect the near-wellbore chemical conditions. Table 1 summarizes selected studies on carbonate dissolution and CO_2–brine interactions and highlights the research gaps addressed in the present study.

The primary aim of the study is to quantify lithology-dependent chemical responses and early-time dissolution behavior under controlled subsurface-like conditions. Thus, this study investigated the dissolution kinetics of carbonate rocks under high-pressure brine and brine–CO_2 conditions relevant to geological CO_2 storage. Controlled static experiments were conducted on limestone and dolomite core plugs to quantify pH evolution, cation release, and early time calcium dissolution rates, providing a direct kinetic comparison across lithologies and fluid conditions. This enables direct assessment of lithology-dependent early reaction behavior under matched experimental conditions. The findings of this study improve our understanding of the geochemical processes that influence subsequent mineralization.

2. MATERIALS AND METHODOLOGY

2.1. Materials. Carbonate rocks are cation-rich, making them a preferred choice for studying the cation dissolution behavior in brine systems relevant to CO_2 mineralization and dissolution processes[8]. Accordingly, two Indiana Limestone and two Maquoketa Dolomite core plugs with nearly identical geometries were selected for this study (Figure 1). The mineralogical differences between the limestone and dolomite samples were confirmed using X-ray diffraction (XRD) and X-ray fluorescence (XRF) analyses[16]. The XRD patterns of the limestone samples showed dominant peaks corresponding to calcite, whereas the dolomite samples exhibited characteristic peaks matching the dolomite reference patterns, confirming the dominant mineral phases in each rock. This interpretation was further supported by the XRF elemental composition (Table 2), which indicates that the limestone samples contain very high Ca content (≈97 wt%) with negligible Mg, whereas the dolomite samples contain significant Mg (≈19 wt%) alongside Ca, consistent with the $CaMg(CO_3)_2$ mineral structure. Together, the XRD and XRF results confirmed the mineralogical differences between the two carbonate lithologies.

The brines were prepared using ACS reagent-grade salts containing NaCl, $CaCl_2$, $MgCl_2$, $NaHCO_3$, and Na_2SO_4. The synthetic brine composition was selected to mimic the major ionic

Table 2. *Elemental composition of the carbonate samples determined by XRF*

Rock type	Ca (wt.%)	Mg (wt.%)	Cl (wt.%)	Al (wt.%)	Fe (wt.%)
Indiana Limestone	97.36	0.2281	0.7899	0.3293	0.3154
Maquoketa Dolomite	78.05	19.41	0.7485	0.3166	1.009

composition of Arabian Gulf seawater and to provide a representative saline environment for investigating carbonate dissolution under CO_2–brine conditions. The composition of the synthetic brine is summarized in Table 3. Prior to the experiments, the synthetic brine had an initial pH of 7.52, establishing the chemical baseline before rock–fluid interaction.

This study used CO_2 gas supplied by Air Liquide, Saudi Arabia, with brine prepared using deionized water.

2.2. Methodology.

2.2.1. Petrophysical properties. The petrophysical properties of the core plugs were measured using a helium porosimeter (HEP-E, VINCI Technologies, Nanterre, France) and a liquid permeameter (LP-100A, Porous Materials Inc., Ithaca, NY, USA) to determine the porosity, grain density, and permeability. The helium porosimeter operates by gas expansion and Boyle's law, and the liquid permeameter measures steady-state single-phase liquid flow through plug-sized core samples. Distilled water was used as the permeating fluid for the liquid permeability measurements, while helium gas was used as the expansion gas for porosity and grain-density determination. The core plugs were used under dry conditions for the porosity measurements and under fully brine-saturated conditions for the permeability measurements[17]. Table 4 summarizes the geometric and petrophysical properties of the limestone and dolomite core samples used in this study.

To perform the liquid permeability measurements, a brine solution (Table 3) was required. The brine was loaded into an accumulator and connected to a permeability pump to prevent corrosion within the pump. Permeability measurements were conducted at flow rates of 1, 2, and 3 cc/min until pressure stabilization was achieved. The pressure drops recorded at each flow rate were used to calculate the permeability, as listed in Table 4.

2.2.2. Test prototypes and experimental parameters. The experimental program consisted of four sealed reaction cells (Figure 5) used to investigate the carbonate dissolution kinetics under controlled brine-only and brine–CO_2 conditions. Each reaction cell contained a single cylindrical carbonate core plug, resulting in four test specimens: two dolomite samples (DL-1 and DL-2) and two limestone samples (LS-1 and LS-2). Two reaction cell geometries were employed: three cells with identical external geometries (Type A) and one cell with a different external shape (Type B). Despite the differences in external geometry, both cell types were designed with identical internal capacities (1000 mL) to ensure consistent fluid volumes and comparable boundary conditions across all experiments.

After the core samples were lowered into the reaction cells, they were filled with a fixed brine volume of 725 mL. In selected experiments, 200 mL of CO_2 was introduced into the reaction cell while maintaining a system pressure of 2000 psi. Under these high-pressure conditions, a significant portion of the injected CO_2 dissolved in the brine, resulting in elevated dissolved CO_2 concentrations. The dissolved CO_2 reacted with water to form carbonic acid (H_2CO_3), which lowered the solution pH and established CO_2–brine conditions representative of subsurface CO_2 storage environments. All the experiments were conducted under static chemical loading with no imposed fluid flow, mechanical loading, or cyclic stress applied to the specimens. Static conditions were selected to isolate the intrinsic chemical kinetics of carbonate dissolution under controlled pressure and temperature conditions. By eliminating fluid flow, transport effects such as advection and dispersion were minimized; thus, the observed changes in pH and dissolved cation concentrations primarily reflected rock–fluid reaction processes. The operating pressure and temperature were maintained at constant values of 2000 psi and 75 °C, respectively, to simulate the subsurface reservoir conditions. A summary of the experimental configurations, including the specimen identifiers, fluid volumes, and operating conditions, is presented in Table 5.

All reaction cells were connected to a high-pressure pumping system to maintain the operating pressure at 2000 psi throughout the experimental period. Following pressurization, the cells

Table 3. *Properties of the synthetic brine*

Ions	Composition (ppm)
Na^+	18,300
$Ca2^+$	650
Mg^{2+}	2,110
SO_4^{2-}	4,290
Cl^-	32,200
HCO_3^-	120
TDS	57,670
pH value	7.52

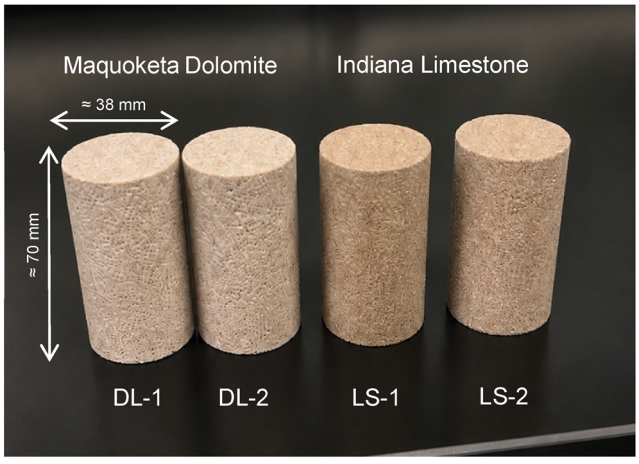

Figure 1. Geometry of core plugs used in this study

Table 4. *Geometric and petrophysical properties of the core plugs*

Sample	Length (mm)	Diameter (mm)	Porosity (%)	Permeability (mD)	Grain Density (g/cc)
LS-1	69.37	38.16	17.75	88	2.692
LS-2	69.3	38.18	17.99	89	2.694
DL-1	70.4	38.25	17.01	75	2.85
DL-2	70.12	38.24	17.04	74	2.827

Table 5. *Summary of experimental conditions for all tests*

Cylinder	Rock ID	Lithology	Brine Volume (ml)	CO_2 Volume (ml)	Pressure (psi)	Temperature (°C)	Cell Geometry
1	DL-1	Dolomite	725	0	2000	75	Type A
2	DL-2	Dolomite	725	200	2000	75	Type A
3	LS-1	Limestone	725	0	2000	75	Type A
4	LS-2	Limestone	725	200	2000	75	Type B

were placed inside a temperature-controlled oven and maintained at 75 °C. Once thermal equilibrium was established, the experiments were initiated and allowed to proceed under static conditions with no imposed fluid flow, mechanical loading, or cyclic stress applied to the specimens. Figure 3 illustrates the experimental setup, with the arrangement of the reaction cells within the temperature-controlled oven and their connection to a common high-pressure manifold for uniform pressure control.

The dissolution behavior was monitored through periodic brine sampling during the experimental runs. At weekly intervals, aliquots of approximately 5–10 mL were withdrawn from each reaction cell and filtered to remove the suspended particulates. pH measurements were performed immediately after sampling to track the temporal evolution of solution chemistry. The pH was measured using a glass-electrode pH probe, with a typical measurement uncertainty of approximately ±0.01 to ±0.05 pH units depending on calibration and probe condition. The filtered samples were subsequently analyzed by ion chromatography (IC) to quantify the dissolved cation concentrations as a function of the reaction time [18]. For the IC measurements, the analytical precision was estimated using a relative standard deviation (RSD) of approximately 1%.

Sampling resulted in a minor pressure loss within the reaction cells; thus, to maintain constant experimental conditions, the system pressure was restored following each sampling event using a high-pressure pump. Distilled water was used for pressure compensation owing to the incompatibility of saline fluids with the pumping system. The injected volumes required for pressure restoration were equal to the withdrawn sample volumes (≈5–10 mL/event), which corresponded to <1.4% of the total brine volume (725 mL). Therefore, the effect of dilution on the system was minimal and did not significantly influence the measured pH or dissolved cation concentration. This procedure ensured that stable pressure was maintained throughout the experimental period.

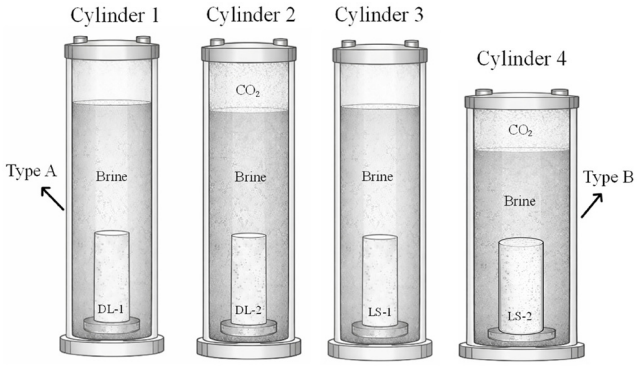

Figure 2. Schematic of the reaction cells and experimental configurations

3. RESULTS AND DISCUSSION

The chemical evolution of carbonate rocks under high-pressure brine and brine–CO_2 conditions reflects the combined effects of CO_2-induced acidification, mineral dissolution kinetics, and progressive buffering under static conditions. Brine-only systems evolve without externally imposed acidity, with their behavior primarily governed by mineral buffering and progression towards chemical equilibrium. By contrast, brine–CO_2 systems exhibit an initial acid-driven response due to carbonic acid formation, followed by gradual neutralization as carbonate dissolution consumes acidity. The mineralogical differences between limestone and dolomite further modulate these responses [11].

3.1. Cation Evolution. Dissolved cation concentrations provide direct evidence of carbonate–fluid interactions, capturing both early-time dissolution kinetics and subsequent chemical equilibration behavior under static conditions [12]. Limestone dissolution is dominated by calcite and typically equilibrates rapidly, whereas dolomite dissolution involves coupled Ca^{2+} and Mg^{2+} release and proceeds more slowly owing to mineral-specific reaction kinetics. Under CO_2-bearing conditions, increased solution acidity enhances the chemical driving force for early-stage dissolution, while progressive neutralization and approach toward saturation limit sustain cation release over time [13].

3.1.1. Dolomite systems. In dolomite-bearing systems under brine-only conditions (Figure 4a), the Ca and Mg concentrations do not follow a simple monotonic trend, indicating that the fluid chemistry evolves progressively during the reaction [14]. As dissolution proceeds, the brine composition changes and the system moves closer to carbonate equilibrium; therefore,

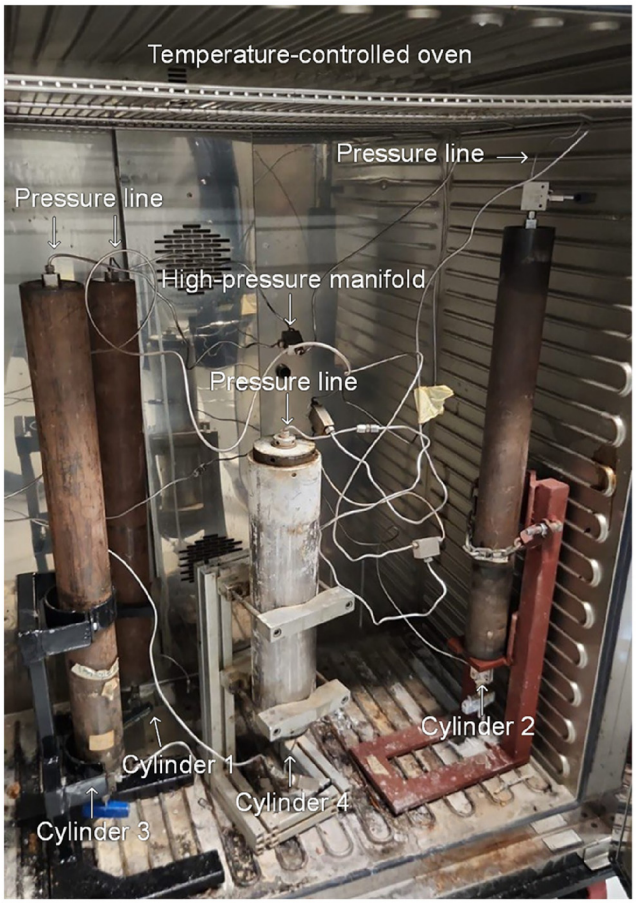

Figure 3. High-pressure, temperature-controlled experimental setup used for dissolution experiments

the measured cation concentrations reflect not only ongoing mineral dissolution but also changing saturation conditions and acid-neutralization effects that can modify the net Ca and Mg response. The observed non-monotonic Ca and Mg behavior may also reflect the evolving saturation conditions and possible carbonate precipitation processes reported in CO_2-reactive carbonate systems[11,19]. Ca starts at very high levels (4.2×10^3 ppm) and drops sharply within the first week (to 1.5×10^3 ppm), whereas Mg rises from a few 10^2 ppm to ~10^3 ppm. This early behavior is consistent with rapid release of Ca^{2+} from the most reactive carbonate surfaces (freshly exposed dolomite faces and/or minor Ca-rich phases such as calcite impurities), followed by rapid removal of Ca^{2+} from the solution as the fluid becomes less undersaturated and secondary Ca-bearing solids begin to form.

The mid-test rebound in Ca (around day 14), alongside relatively steady Mg, suggests episodic re-exposure of the reactive surface area combined with intermittent precipitation control of Ca^{2+}.

The late stage is characterized by extremely low Ca (near a few 10^2ppm), whereas Mg peaks (~1.9×10^3ppm) before collapsing by the final sampling point. This pattern is consistent with an incongruent carbonate reaction, where Ca is preferentially removed from the solution (most commonly by calcite or Ca-rich carbonate precipitation), whereas Mg accumulates until Mg-bearing carbonates begin to limit Mg^{2+}, driving the terminal Mg drop[20].

Under brine–CO_2 conditions (Figure 4b), the process is more chemically directed. Ca decreases steadily from 2.3×10^3ppm to 3–4 $\times 10^2$ppm, whereas Mg increases from 6×10^2ppm to 1.6×10^3ppm. The dissolved CO_2 forms carbonic acid, which lowers the pH and sustains carbonate dissolution. Under these conditions, the system experiences stronger dissolution kinetics and a larger reactive zone than CO_2-free brine at the same pressure and temperature. The continued decline in Ca, despite acid-driven dissolution, implies the efficient removal of Ca by secondary sinks during the reaction. In contrast, Mg^{2+} is less rapidly scavenged and accumulates in the solution, leading to an increased Mg/Ca ratio in the final stage. Mechanistically, this behavior reflects a CO_2-driven dissolution front accompanied by near-surface precipitation, which suppresses Ca in the bulk brine while allowing Mg to track the ongoing dolomite reaction more directly.

3.1.2. Limestone systems. In limestone–brine systems (Figure 5a), Ca starts at relatively high level (≈2000 ppm) and trends downward overall, with a small mid-term rebound (dropping to ≈1600 ppm after approximately one week, rising to ≈1800 ppm at approximately two weeks, then declining to a few hundred ppm by ~35 days). Mg increases to a peak (≈1200–1300 ppm at ~two weeks), remains stable through ~three to four weeks (≈1100–1200 ppm), and then drops sharply near the end. This behavior reflects a transition from early net ion release to late-stage removal from the solution, with Ca decreasing sooner and more strongly than Mg.

In the presence of CO_2 (Figure 5b), the system exhibited stronger transients. Ca concentration started at ~2200 ppm, decreased rapidly (~1000 ppm by ~10 days), rebounded (~1800 ppm by ~17 days), and declined to ~500–600 ppm by ~38 days. Mg mirrored this dip–rebound–decline pattern. Compared with brine-only conditions, CO_2 produced larger excursions and faster early changes. This is consistent with CO_2-driven acidification enhancing early carbonate reactivity, followed by progressive stabilization, where both Ca and Mg decrease simultaneously. The late convergence of Ca and Mg suggests that long-term control involves coupled processes that affect both cations rather than simple calcite dissolution alone.

3.2. pH Evolution. Under CO_2-rich conditions, the dissolved CO_2 reacts with water to form carbonic acid, which promotes carbonate dissolution and contributes to acid neutralization. The primary dissolution reactions can be represented as follows:

$$CaCO_3 + CO_2 + H_2O \rightarrow Ca^{2+} + 2HCO_3-$$

$$CaMg(CO_3)_2 + 2CO_2 + 2H_2O \rightarrow Ca^{2+} + Mg^{2+} + 4HCO_3-$$

These reactions illustrate how calcite and dolomite dissolution consume acidity while releasing dissolved cations into the solution. Accordingly, the pH evolution reflects the balance between CO_2-derived acidity and carbonate buffering. Brine-only systems are expected to exhibit a stable or increasing pH as carbonate dissolution consumes protons, whereas brine–CO_2 systems initially exhibit suppressed pH, followed by recovery as acid-neutralization reactions dominate. Owing to the distinct buffering capacity between limestone and dolomite, pH trends must be interpreted across all systems and within individual

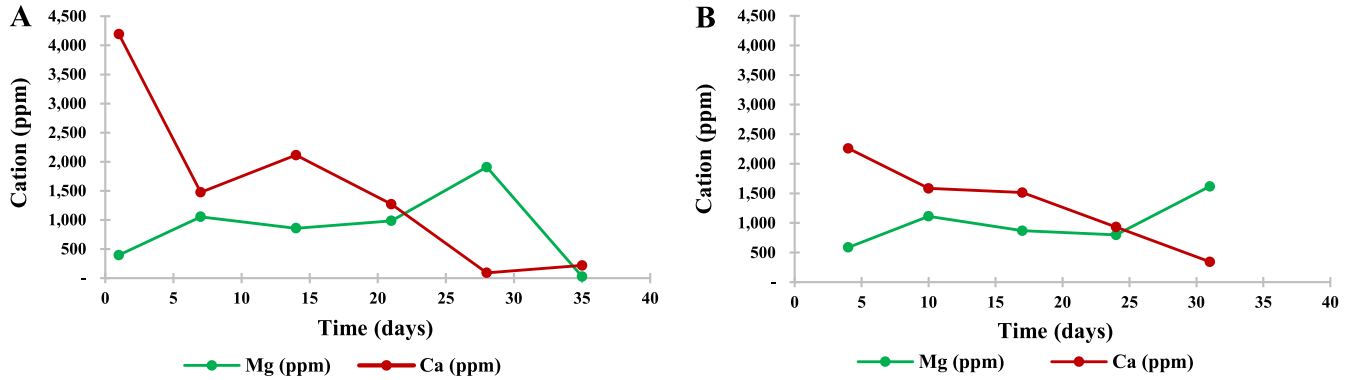

Figure 4. Ca^{2+} and Mg^{2+} in dolomite systems under (a) brine-only and (b) brine–CO_2 conditions

lithologies. Although a fixed CO_2 volume (200 mL) was introduced into the reaction cell, solution acidity is primarily governed by the resulting CO_2 partial pressure (pCO_2) under the maintained system pressure of 2000 psi. The injected CO_2 volume mainly establishes CO_2-rich conditions, whereas the chemical behavior of the system is governed by the elevated pCO_2 and the resulting formation of carbonic acid.

For dolomite (Figure 6a), a strong time-dependent neutralization trend was observed. In brine-only, pH was initially ≈5.2 at ~7 days and rose steadily to near-neutral/weakly alkaline values (≈7.0 by ~21 days and ≈7.3 by ~35 days), consistent with progressive dolomite buffering. In the brine–CO_2 condition, the measured pH was already higher at the first sampling point (≈6.35 at ~10 days) and then climbed to ~7.2–7.3 by ~24–31 days, implying faster early acid neutralization in the presence of CO_2, followed by a plateau as the system approached carbonate equilibrium.

In contrast, the limestone systems (Figure 6b) exhibited considerably greater pH stability. In brine-only, pH remained at approximately 6.6–6.8 from ~7 to ~35 days, indicating rapid establishment of a near-steady carbonate equilibrium. In brine–CO_2, only a modest mid-term acidification was observed (≈6.5 at ~24 days), followed by recovery toward ~6.9–7.0 by ~31–38 days, consistent with temporary CO_2-driven acidification and subsequent buffering by calcite dissolution.

Overall, the key distinction lies in both amplitude and kinetics. Dolomite exhibits a large pH swing over weeks, signaling slower but stronger cumulative buffering, whereas limestone remains near neutral throughout, showing rapid buffering and early stabilization with only small CO_2-driven perturbations. At the end, both systems become nearly neutral, but dolomite maintains a slightly higher pH (7.2–7.3) than limestone (6.9–7.0).

3.3. Quantitative Evaluation of Dissolution Kinetics.

To compare the carbonate dissolution kinetics across lithologies and fluid compositions quantitatively, early-time Ca^{2+} release rates were derived from the measured concentration–time data. Calcium was selected as the primary kinetic tracer because of its direct stoichiometric association with carbonate mineral dissolution in both the limestone and dolomite systems.

3.3.1. Early-time Ca^{2+} release rates. The initial dissolution behavior was quantified using the early-time slope of the Ca^{2+} concentration–time curve, defined in Eq. (1).

$$R_{Ca,0} = \frac{\Delta C_{Ca}}{\Delta t} \tag{1}$$

where C_{Ca} is the dissolved calcium concentration (ppm) and t is the time (days). The slopes were calculated using the first two sampling points to capture the initial kinetic responses of the system. Later, progressive acid neutralization, chemical equilibration, and potential secondary precipitation processes began to influence the measured cation concentrations, implying that the system no longer reflected the initial dissolution behavior purely. Therefore, the first concentration interval provided the most representative estimate of the initial dissolution

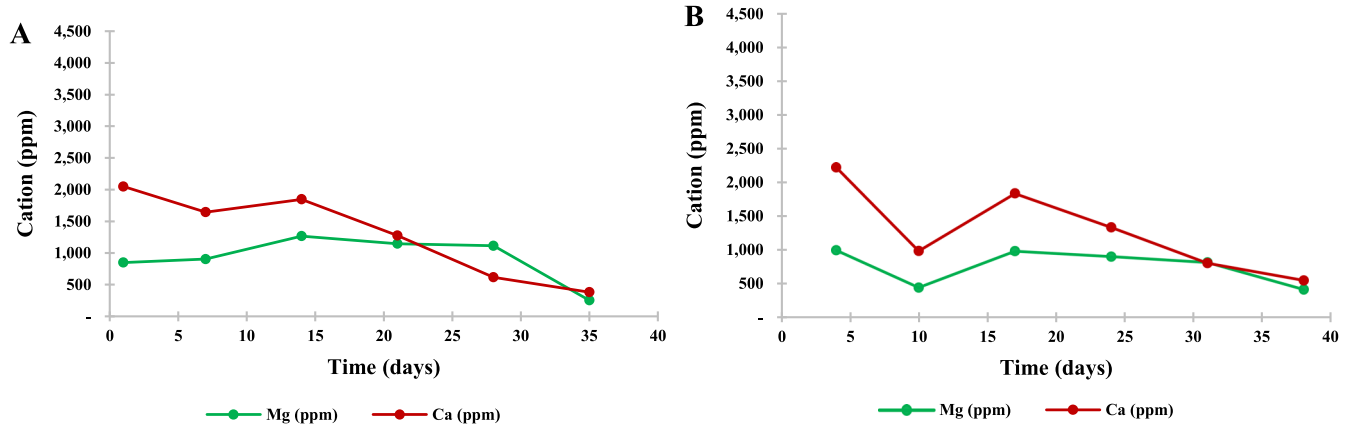

Figure 5. Ca^{2+} and Mg^{2+} in limestone systems under (a) brine-only and (b) brine–CO_2 conditions

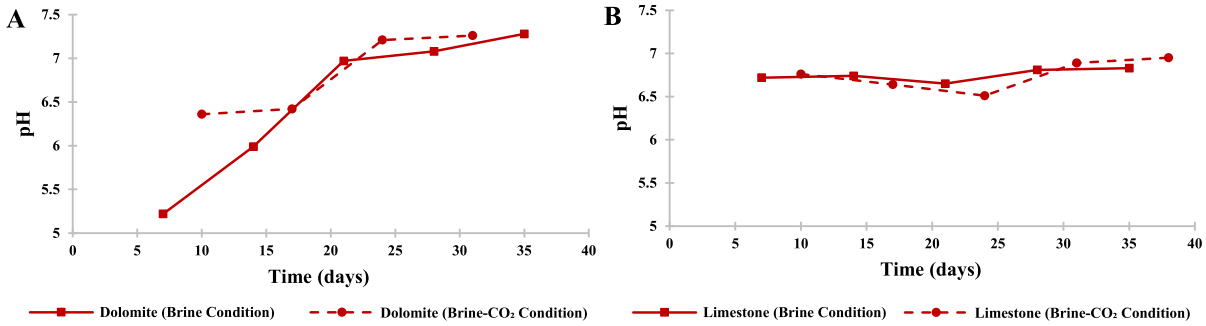

Figure 6. pH evolution for dolomite (a) and limestone (b) samples under brine-only and brine–CO_2 conditions

Table 6. *Early-time Ca^{2+} dissolution slopes and surface-area normalized dissolution rates*

Cylinder	Lithology	Condition	Early-time slope (ppm · day^{-1})	$r_{Ca,0}$ (mol · m^{-2} · day^{-1})
1	Dolomite	Brine	-452.9	-0.773
2	Dolomite	Brine–CO_2	-112.6	-0.192
3	Limestone	Brine	-67.4	-0.115
4	Limestone	Brine–CO_2	-205.0	-0.350

rate before the secondary processes affected the chemical evolution of the system. The calculated early-time slopes (Table 6) show clear lithology- and CO_2-dependent contrasts. The negative sign of the slope indicates a net decrease in the dissolved Ca^{2+} concentration over time, reflecting rapid early-stage chemical adjustment, followed by progressive solution neutralization and secondary-process control. Moreover, the dolomite brine-only system exhibited the largest slope, indicating the most rapid initial chemical adjustment. The limestone systems displayed smaller early-time slopes, consistent with faster equilibration and a weaker pH buffering capacity relative to dolomite. Notably, the presence of CO_2 suppressed the magnitude of the early-time Ca^{2+} decline in dolomite, while substantially increasing early calcium mobilization in limestone.

3.3.2. Surface-area normalized dissolution rates. To enable a direct comparison of dissolution kinetics independent of specimen size, Ca^{2+} release rates were normalized to the exposed geometric surface area of each core plug, according to Eq. (2).

$$r_{Ca,0} = \frac{1}{A}\frac{dn_{Ca}}{dt} \tag{2}$$

where n_{Ca} is the number of moles of dissolved calcium calculated from the measured concentrations and fixed brine volume (0.725 L), and A is the geometric surface area of the cylindrical core plug determined from the measured dimensions (Table 4). The geometric surface area was used as a consistent normalization basis for all specimens, recognizing that the effective reactive surface area may differ owing to pore-scale roughness and mineral heterogeneity.

The resulting surface-area normalized dissolution rates (Table 6) confirmed that dolomite exhibited higher effective dissolution rates than limestone under brine-only conditions. CO_2 modified the dissolution kinetics in a lithology-dependent manner, reducing the apparent initial dissolution rate in dolomite and enhancing early calcium release in limestone [15]. These contrasts indicate that the early reaction stage is kinetically controlled and strongly influenced by the mineralogy and fluid composition [19]. Collectively, these findings demonstrate that the early-stage cation release plays a critical role in regulating both CO_2 solubility enhancement and the initiation of mineral trapping in carbonate reservoirs. From a CCS perspective, the results emphasize that short-term dissolution kinetics can strongly influence the timing and extent of mineralization, particularly in systems where Ca^{2+} and Mg^{2+} availabilities limit carbonate formation. These results are consistent with previous studies showing that carbonate dissolution behavior depends strongly on mineralogy and CO_2-related reaction conditions, while the present work extends this understanding through a direct early-time core-scale comparison between limestone and dolomite under controlled brine-only and brine–CO_2 conditions. Therefore, incorporating early-time kinetic behavior into reactive transport and reservoir-scale models is essential for improving the prediction of long-term CO_2 storage security. Future work should extend this framework to flowing systems and longer reaction times to better represent field-scale conditions and mineralization potential.

4. CONCLUSIONS

This study examined the dissolution kinetics of carbonate rocks under high-pressure brine and brine–CO_2 conditions relevant to geological CO_2 storage and mineralization. Through controlled core-scale experiments and time-resolved measurements of pH and dissolved cation concentrations, this work provides quantitative insights into the early-stage mineral–fluid interactions that govern CO_2 trapping behavior in carbonate reservoirs.

The following conclusions were drawn:

1. The experimental systems exhibited systematic and reproducible pH and cation evolution, demonstrating that the applied pressure–temperature conditions and static experimental design are well-suited for isolating the early-time dissolution behavior.

2. Carbonate lithology strongly controlled the chemical response, with dolomite displaying a greater buffering capacity and more sustained cation release than limestone. This reflects

the fundamental differences in mineral composition and dissolution kinetics.

3. The presence of CO_2 significantly modified the early-stage dissolution behavior by lowering the initial pH and altering the calcium release in a lithology-dependent manner, thereby directly influencing the short-term availability of divalent cations for mineralization.

4. Quantified early-time Ca^{2+} dissolution rates indicate that the initial CO_2–brine–rock interactions are predominantly kinetics-controlled, preceding progressive acid neutralization and partial chemical equilibration.

The present results suggest that early-time lithology-dependent dissolution and cation release may influence CO_2 buffering, the onset of mineral trapping, and geochemical evolution in carbonate storage systems. However, several limitations should be acknowledged: The experiments were conducted on a limited number of four core-scale samples (~70 mm in length). Furthermore, the experiments were performed under static conditions with no imposed fluid flow and over a limited duration of approximately 35–38 days.

In natural reservoirs, additional processes, such as fluid flow, larger spatial heterogeneity, and much longer reaction times (years to decades), may influence rock–fluid interactions. Therefore, the results represent laboratory-scale observations of early dissolution kinetics and provide insight into processes relevant to CO_2 storage, whereas direct extrapolation to reservoir-scale behavior requires further investigation.

AFFILIATIONS AND AUTHOR DETAILS

Undergraduate Author

Turki Aljuaid – *Department of Petroleum Engineering, King Fahd University of Petroleum & Minerals, Dhahran 31261, Saudi Arabia*; 0009-0000-9540-1111
Email: s202245360@kfupm.edu.sa

Corresponding Author

Dhafer Al Shehri – *Research Mentor, Associate Professor, Department of Petroleum Engineering, King Fahd University of Petroleum & Minerals, Dhahran 31261, Saudi Arabia*; 0000-0002-7032-5199
Email: alshehrida@kfupm.edu.sa

ACKNOWLEDGEMENTS

The authors gratefully acknowledge the support of the Department of Petroleum Engineering and the Center for Integrative Petroleum Research (CIPR) at King Fahd University of Petroleum and Minerals. The authors also thank the technical staff and laboratory team, with special appreciation to Eng. Ammar Al-Ramdhan, for their assistance with specimen preparation and experimental testing. The authors further acknowledge Dr. Isah for his support and guidance throughout this work.

REFERENCES

(1) CATF. Carbon capture and storage: What can we learn from the project track record? 2024.

(2) Weijermars, R. Concurrent challenges in practical operations and modeling of geological carbon-dioxide sequestration: Review of the Gorgon project and FluidFlower benchmark study. *Energy Strategy Rev.* **56**, 101586 (2024).

(3) De Jonge-Anderson, I. *et al.* Regional screening of saline aquifers in the Malay Basin for CO_2 storage. *Int. J. Greenh. Gas Control* **143**, 104347 (2025).

(4) Orivri, U. D., Chanda, P., Johnson, L., Koehn, L. W. & Pollyea, R. M. Opportunities and challenges for geologic CO_2 sequestration in carbonate reservoirs: A review. *Int. J. Greenh. Gas Control* **142**, 104342 (2025).

(5) Bashir, A. *et al.* Comprehensive review of CO_2 geological storage: Exploring principles, mechanisms, and prospects. *Earth-Sci. Rev.* **249**, 104672 (2024).

(6) Massarweh, O. & Abushaikha, A. S. CO_2 sequestration in subsurface geological formations: A review of trapping mechanisms and monitoring techniques. *Earth-Sci. Rev.* **253**, 104793 (2024).

(7) Kelemen, P., Benson, S. M., Pilorgé, H., Psarras, P. & Wilcox, J. An Overview of the Status and Challenges of CO_2 Storage in Minerals and Geological Formations. *Front. Clim.* **1**, 9 (2019).

(8) Kim, K., Kim, D., Na, Y., Song, Y. & Wang, J. A review of carbon mineralization mechanism during geological CO_2 storage. *Heliyon* **9**, e23135 (2023).

(9) Fentaw, J. W. *et al.* Integrated Geochemical Modeling of Trapping Mechanisms and Sensitivity Analysis for Optimized CO_2 Sequestration in Saline Aquifers. *ACS Omega* **10**, 53417–53437 (2025).

(10) Cicha-Szot, R., Labus, K. & Leśniak, G. Pore-Scale Evolution of Carbonate and Sandstone Reservoirs Under CO_2–Brine Interaction: Implications for Sustainable Carbon Storage. *Sustainability* **17**, 9102 (2025).

(11) Luquot, L. & Gouze, P. Experimental determination of porosity and permeability changes induced by injection of CO_2 into carbonate rocks. *Chem. Geol.* **265**, 148–159 (2009).

(12) Yang, Y. *et al.* Dynamic Pore-Scale Dissolution by CO_2 - Saturated Brine in Carbonates: Impact of Homogeneous Versus Fractured Versus Vuggy Pore Structure. *Water Resour. Res.* **56**, e2019WR026112 (2020).

(13) Morse, J. W., Arvidson, R. S. & Lüttge, A. Calcium Carbonate Formation and Dissolution. *Chem. Rev.* **107**, 342–381 (2007).

(14) Arvidson, R. S., Fischer, C. & Luttge, A. Calcite Dissolution Kinetics: A comment upon "Evidence and Potential Implications of Exponential Tails to Concentration Versus Time Plots for the Batch Dissolution of Calcite by V. W. Truesdale". *Aquat. Geochem.* **21**, 415–422 (2015).

(15) Briolet, T., Bemer, E., Sissmann, O. & Fortin, J. Localized versus distributed dissolution in carbonate rocks: The key role of microstructure. *Geochim. Cosmochim. Acta* **397**, 113–133 (2025).

(16) Helmi, M. E., Mohammed, I., Adebayo, A. R., Abdelgawad, K. Z. & Mahmoud, M. Geoelectrical Evaluation of CO_2 Storage in Carbonate Aquifers Using Carbonated Water Injection. *Energy Fuels* **39**, 18969–18979 (2025).

(17) Abu-Khamsin, S. A. Basic Properties of Reservoir Rocks; King Fahd University of Petroleum & Minerals: Dhahran, Saudi Arabia 2004.

(18) Michalski, R. Ion Chromatography Applications in Wastewater Analysis. *Separations* **5**, 16 (2018).

(19) Pokrovsky, O. S., Golubev, S. V. & Schott, J. Dissolution kinetics of calcite, dolomite and magnesite at 25 °C and 0 to 50 atm pCO_2. *Chem. Geol.* **217**, 239–255 (2005).

(20) Zhu, C. & Lu, P. Alkali feldspar dissolution and secondary mineral precipitation in batch systems: 3. Saturation states of product minerals and reaction paths. *Geochim. Cosmochim. Acta* **73**, 3171–3200 (2009).